



# Molecular modelling approach of Novel Oxazine substituted 9- anilinoacridine as ER $\alpha$ inhibitors Targeting Breast cancer

Potlapati Varakumar<sup>1</sup>, Dr. Kalirajan Rajagopal<sup>1\*</sup>, Baliwada Aparna<sup>1</sup>, Kannan raman<sup>1</sup> and Gowramma Byran<sup>1</sup>

<sup>1</sup>Department of Pharmaceutical Chemistry, JSS College of Pharmacy (JSS Academy of Higher Education & Research), Ooty, The Nilgiris, Tamil Nadu, India.

Corresponding Author: rkalirajan@ymail.com, rkalirajan@jssuni.edu.in

## Abstract

The mammary epithelium contains the oestrogen receptor alpha (ER $\alpha$ ), which is crucial for the development of breast cancer and endocrine therapy. The majority of breast cancers about two thirds overexpress ER $\alpha$ , making them more responsive to hormone therapy and giving them a better prognosis than tumours that express ER $\alpha$  infrequently or not at all. Anti-estrogens have been demonstrated to prevent the growth of breast cancer cells by out-competing oestrogen for binding to nuclear receptors. The tumour grow in response to the oestrogen hormone are termed as ER-Positive breast cancer. The majority of breast cancers about 80% are ER-positive. Because of their ability to inhibit cell proliferation, 9-aminoactridines are important DNA-intercalating agents. The Schrodinger suit's Prime-MM-GB/SA module does binding free energy calculations, the Glide module conducts in-silico ADMET screening, and the QikProp module performs molecular docking studies for the 26 designed compounds 1a–z. Based on the GLIDE score, the binding affinity of the created compounds 1a–z towards ER was selected. As compared to the industry benchmarks Tamoxifen (-11.58) and Ledacrine (-12.84), the compounds 1a-z, aside from 1x and 1u, have substantial Glide scores in the range of -12.91 and -12.84. (-7.93). A 100ns MD simulation was performed on compound 1x against protein 2IOG.pdb. This study offers support for the idea of novel 9-anilinoacridine compounds with oxazine substitutions as possible ER inhibitors. Further in-vitro and in-vivo studies may demonstrate the therapeutic potential of the compounds, 1x, u with significant Glide scores, which may result in significant anti-breast cancer activity.

**Keywords:** 9-anilinoacridine, Oxazine, ER $\alpha$ , Molecular Modelling, Breast cancer.

## INTRODUCTION

One of the most often diagnosed malignancies in women is breast cancer. It should be noted that 70% of breast cancer diagnoses are ER $\alpha$ +, making it a crucial therapeutic target. As a result, the two ER subtypes, ER $\alpha$  and ER $\beta$ , affect breast cancer cells in very different ways. The ER $\beta$  isoform displays inhibitory effects on the same carcinogenic activities while ER $\alpha$  enhances them.<sup>1</sup> The FDA-approved medications tamoxifen,<sup>2</sup> toremifene, raloxifene, and fulvestrant, which all bind to the oestrogen binding site of the receptor, were discovered through ER-directed small molecule drug discovery for breast cancer. These non-selective ER-directed inhibitors may eventually cause resistance in breast cancer cells and raise the possibility of endometrial cancer growth. Thus, it is imperative to create new medications with alternative ER $\alpha$  targeting mechanisms that can get around the drawbacks of traditional anti-ER $\alpha$  therapy. Recently, the DNA binding domain (DBD), a functional region on the ER $\alpha$ , has been thought of as a potential target in the context of drug discovery.<sup>3</sup>

Chemotherapy is frequently the preferred course of treatment for many cancer types, and developing novel chemotherapeutic drugs continues to be crucial to the war on cancer. Using substances that interact with DNA or block enzymes necessary for cell survival and replication is a plausible strategy in this field. One such substance is amsacrine, a popular antiproliferative drug used to treat various malignancies, including acute adult leukaemia. The poisoning of ER activity prevents the process of relegation and results in fatal double-strand DNA breaks, which cause cell cycle arrest and apoptosis. The planar aromatic system of the acridine moiety was referred to as having the intercalative property.<sup>4</sup>

The most well-known member of the 9-anilinoacridines family is amsacrine. It was one of the first DNA-intercalating compounds to be evaluated as a topoisomerase II inhibitors.<sup>5</sup> In substances with sufficiently big coplanar aromatic chromophores, the intercalation process is the strongest sort of reversible binding to the double helix DNA. The manner of binding is significant, as the chromophore intercalates with the DNA base pairs, according to several thorough SAR analyses of acridine-based DNA-intercalating agents.<sup>6</sup> As a result of the chemical alterations made to acridines, such as the addition of various substitutions or heterocyclic rings, research on the structure-activity connections has been expanded, providing fresh information on molecular interactions at the receptor level. In fact, it is widely known that 9-anilinoacridines

with minor structural changes may have a variety of pharmacological effects. Oxazine derivatives exhibit a variety of biological activities, including antibacterial and anticancer properties. In order to find the affinities and interactions responsible for ER $\alpha$  inhibitions, 9-anilinoacridine analogues bearing the oxazine residue on aniline rings were constructed by molecular docking studies using Schrodinger suit LLC. There are various modules such as Glide, Qikprop, Prime MM-GBSA, etc. involved in computational methods like docking, ADMET screening, binding energy calculations, etc. The *in-silico* investigations will outline the essential structural elements needed to build a powerful medication.<sup>7</sup>

## MATERIALS AND METHODS

### Protein Preparation

The protein structure in this work was modelled using the crystal structure of protein estrogen receptor alpha (PDB ID: 2IOG) at 2.25 Å, which came from the Protein Data Bank download (PDB). In general, the bond ordering, formal charges, missing hydrogen atoms, topologies, and incomplete and terminal amide groups of protein structures are refined.

5Å of the hetero atom, the water molecules were eliminated. For the heteroatom found in the protein structure, potential ionisation states were produced, the state that was the most stable was chosen. The hydrogen bonds were allocated, and the retained water molecules orientations were adjusted. In order to realign side-chain hydroxyl groups and prevent any steric conflicts, a constrained reduction of the protein structure was completed using the OPLS 5 force field. A predetermined Root Mean Square Deviation (RMSD) threshold of 0.3Å limits the minimization to the supplied protein coordinates.<sup>8</sup>

### Ligand Preparation

The ligand structures were created in CDX format using Chem Draw Ultra version 8.0. The Schrodinger suit 2013 then converted these ligands to the mol 2 format and subjected them to the LigPrep module. They were converted from 2D to 3D structures by adding stereochemistry, ionisation, tautomeric variations, energy minimization, optimising for geometry, desalting, and correcting for chiralities and missing hydrogen atoms. These ligands had predefined bond ordering, and the charged groups were neutralised. The ionisation and tautomeric states were created between pH 6.8

and 7.2 using the Epik module. Using the Impact package of Schrodinger's Optimal Potentials for Liquid Simulations-2003 (OPLS-3) force field, chemicals were reduced in LigPrep's last stage until a root mean square deviation of 2.5Å<sup>o</sup> was reached. For minimization, the steepest descent technique was utilised, then the conjugate gradient method. The optimised ligands were employed for docking studies, and a single low energy ring confirmation was obtained for each ligand.<sup>9</sup>

### **Receptor grid generation**

The generated proteins crystal structure was used to build the receptor grid, contained the ligand. The proteins binding box dimensions were set to 11Å<sup>o</sup> × 12Å<sup>o</sup> × 12Å<sup>o</sup>. (within which the centroid of a docked posture is contained).

### **Validation of the docking programme**

The degree to which an experimental binding mode identified by X-ray crystallography resembled the co-crystallized ligand's lowest energy pose (binding conformation), predicted by the object scoring functions, Glide score (G Score), was used to assess the accuracy of the docking technique. By taking the co-crystallized ligand out of the binding site, the extra precision Glide docking method was proven to be effective. Results were analysed using the interactions between hydrogen bonds and the root mean square deviation (RMSD) between the expected confirmation and the observed X-ray crystallographic conformation.

### **Glide Ligand docking**

Using the previously created receptor grid and the ligand molecules, the proposed molecules were glide docked. Using the Glide ligand docking tool, the favourable contacts between the ligand molecules and the receptor were graded. OPLS-2005 force field and extra precision (XP) mode were used for all docking calculations. Flexible docking mode, which automatically creates conformations for each input ligand, was used to execute the docking process described above. A number of hierarchical filters that assess the ligand's interaction with the receptor were applied to the generated ligand poses. The initial filter evaluates the complementarity of the ligand-receptor interactions using a grid-based method based on the empirical ChemScore function and tests the spatial fit of the ligands to the designated active site. This approach penalises steric collisions while recognising advantageous hydrophobic, hydrogen-bonding, and metal-ligation interactions. Poses that pass these

first screenings move on to the algorithm's last stage, which entails evaluating and minimising the energy of an approximate grid-based OPLS ligand-receptor interaction. The shortened poses were then rescored using the scoring feature of Glide Score.

The fitness scores for each ligand in the ER $\alpha$  were compared along with the XP-Glide scores of the active molecules. Most of the proposed compounds had positive Glide scores when compared to a reference compound containing the acridine derivative ledacrine, which is a powerful ER $\alpha$  inhibitor and anti-cancer drug.<sup>10</sup>

### ***in-silico* ADMET screening**

The recommended ligands L1–L15 have their *in-silico* ADMET characteristics estimated using the Schrodinger suit 2019-4s Qikprop module. The ligands were run through the Qikprop module to obtain the ADMET parameters, including such molecular weight, dipole moment, the number of H-bond donors and acceptors, logP values, rule of five violence, oral absorption, etc.

### **Binding Free Energy Calculation by Using Prime/MM-GBSA Approach**

Molecular Mechanics-Generalized Born Surface Area is utilised to process the binding free energies of the protein ligand complex in the Schrodinger suite 2019-4s Prime module (MM-GBSA). Using the generalized-Born/surface area (GB/SA) continuum VSGB 2.0 solvent model and the XP docked pose of the ligand receptor complex, the OPLS3 force field was employed to minimise energy.<sup>11</sup>

### **Molecular dynamics (MD) simulations**

100 ns MD simulation research was used to look at the stability of the docked 1x/2IOG complex. Using the Desmond module of Schrodinger 2019-4, the complex in the explicit solvent system with OPLS3 force field was investigated. Under orthorhombic periodic boundary conditions, the molecular system was solvated with crystallographic water (TIP3P) molecules for 10 Å buffer region. By deleting the overlapping water molecules and adding Na as counterions, the solution was made neutral. There are 9363 water molecules and 32153 atoms in the entire system. The systems were kept at a constant temperature (300 K) and pressure (1 bar) using an ensemble (NPT) of Nose-Hoover thermostat and barostat. The use of conjugate gradient techniques followed by a hybrid energy minimization strategy with 1000 steps of steepest descent was made. For energy minimization, another algorithm was

used: the limited memory Broyden-Fletcher-Goldfarb-Shanno (LBFGS) algorithm with a convergence threshold gradient of 1 kcal/mol/ $\text{\AA}^0$ . For estimating long-range electrostatic interactions with a cut-off radius 2 of 9  $\text{\AA}^0$  and short-range van der Waals and Coulomb interactions, the Smooth Particle Mesh Ewald method was applied. The dynamics investigation for bonded, close, and far-bonded interactions with 2, 2, and 6 fs, respectively, using multiple time step RESPA integration (reference system propagator techniques). Data were gathered every 100 ps, and Maestro graphical interphase was used to analyse the acquired trajectory.<sup>12</sup>

## RESULTS AND DISCUSSION

A developed sub-atomic docking programme Schrodinger suit 2019-4 was used to determine the coupling affinities of the ligands by performing sub-atomic docking examinations of the intended molecules to the protein dynamic destinations. Many in-silico research are carried out against cancer targets from the writing works.<sup>13</sup> The structural analogues are docked to the ER $\alpha$  (2IOG) to determine how the ER $\alpha$  inhibits the progression of breast cancer. When compared to conventional acridine subsidiary with anticancer movement ledacrine and against breast cancer specialist tamoxifen, the compounds 1a–z (Figure 1) showed great receptor affinity.

### Figure 1. Structure of compounds 1a-z

Table 1 displays the Glide scores from docking studies against the ER receptor (PDB id 2IOG). With the exception of 1x and 1u, compounds 1a through z exhibit substantial Glide scores in the range of -12.91 and -12.84 when compared to the benchmarks Tamoxifen (-11.58) and Ledacrine (-7.93). Due to the existence of rings like acridine and heterocyclic rings, the docking results show that the binding affinity is primarily caused by lipophilic components. In docking scores in the majority of the mixes, lipophilic factors play a significant role. The LYS724 to LEU 852 buildups,

which are the active site area, are practically overwhelming the cooperatives. (Figure 2)

**Table 1.** Docking studies for Compounds 1a-z with ER $\alpha$  (2IOG)

| Compound        | Glide score | Lipophilic EVdW | Phob En | H Bond | XP Electro | Low MW | XP Penalties | Rot penal |
|-----------------|-------------|-----------------|---------|--------|------------|--------|--------------|-----------|
| 1x              | -12.91      | -8.92           | -2.7    | -0.67  | -0.35      | 0      | 0            | 0.13      |
| 1u              | -12.84      | -8.87           | -2.7    | -0.67  | -0.33      | 0      | 0            | 0.12      |
| 1r              | -11.83      | -8.42           | -2.2    | -0.65  | -0.32      | 0      | 0            | 0.15      |
| 1s              | -11.31      | -7.36           | -2.7    | -0.63  | -0.34      | 0      | 0            | 0.15      |
| 1n              | -10.51      | -9.16           | -2.7    | -0.55  | -0.2       | 0      | 2.4          | 0.16      |
| 1c              | -10.37      | -8.9            | -2.7    | -0.58  | -0.28      | 0      | 2.4          | 0.13      |
| 1p              | -10.31      | -9.11           | -2.7    | -0.42  | -0.22      | 0      | 2.4          | 0.18      |
| 1k              | -10.17      | -8.43           | -2.7    | -0.53  | -0.26      | 0      | 2.4          | 0.16      |
| 1h              | -10.12      | -8.65           | -2.7    | -0.49  | -0.34      | 0      | 2.4          | 0.16      |
| 1f              | -10.08      | -8.78           | -2.7    | -0.54  | -0.2       | 0      | 2.4          | 0.17      |
| 1g              | -9.88       | -8.32           | -2.7    | -0.7   | -0.29      | 0      | 2.4          | 0.16      |
| 1i              | -9.84       | -8.91           | -2.7    | -0.05  | -0.26      | 0      | 2.4          | 0.16      |
| 1y              | -9.78       | -8.94           | -2.7    | -0.04  | -0.2       | 0      | 2.4          | 0.14      |
| 1m              | -9.63       | -8.4            | -2.7    | -0.32  | -0.29      | 0      | 2.4          | 0.16      |
| 1j              | -9.44       | -8.43           | -2.7    | -0.11  | -0.14      | 0      | 2.4          | 0.16      |
| 1a              | -9.39       | -8.51           | -2.7    | -0.14  | -0.13      | 0      | 2.4          | 0.13      |
| 1e              | -9.38       | -8.6            | -2.7    | 0      | -0.16      | 0      | 2.4          | 0.17      |
| 1v              | -9.37       | -7.77           | -2.7    | -0.68  | -0.26      | 0      | 2.4          | 0.12      |
| 1d              | -9.17       | -8.36           | -2.7    | -0.09  | -0.14      | 0      | 2.4          | 0.17      |
| 1z              | -9.11       | -8.38           | -2.7    | -0.7   | -0.43      | 0      | 3.4          | 0.12      |
| 1t              | -9.04       | -8.08           | -2.7    | -0.06  | -0.18      | 0      | 2.4          | 0.12      |
| 1o              | -8.83       | -8.02           | -2.7    | 0      | -0.07      | 0      | 2.4          | 0.18      |
| 1b              | -8.26       | -7.54           | -2.7    | 0      | -0.11      | 0      | 2.4          | 0.13      |
| 1l              | -6.8        | -8.47           | -2.7    | 0      | -0.07      | 0      | 4.8          | 0.15      |
| Tamoxifen (Std) | -11.58      | -8.97           | -2.7    | 0      | -0.06      | -0.26  | 0            | 0.42      |
| Ledacrine       | -7.93       | -5.68           | -2.14   | 0      | 0          | -0.42  | 0            | 0.31      |

|       |  |  |  |  |  |  |  |  |
|-------|--|--|--|--|--|--|--|--|
| (Std) |  |  |  |  |  |  |  |  |
|-------|--|--|--|--|--|--|--|--|

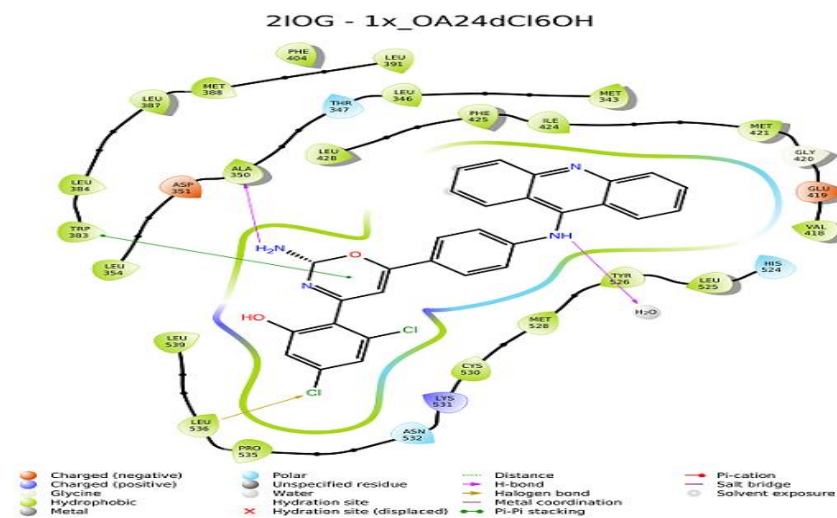


**Figure 2.** Ligand interaction of compound 1x with ER $\alpha$  (2IOG)

The designed ligands' docked postures are displayed in (Figure 3). The majority of 9-anilinoacridine rings with oxazine substitutions can be located in hydrophobic pockets. The compounds 1x, u,r,s,n,c,p,k,h,f with the highest Glide scores have the finest docked postures, which are displayed in (Figure 4). The ligand **1x** exhibited hydrogen bonding as shown in (Figure 5).

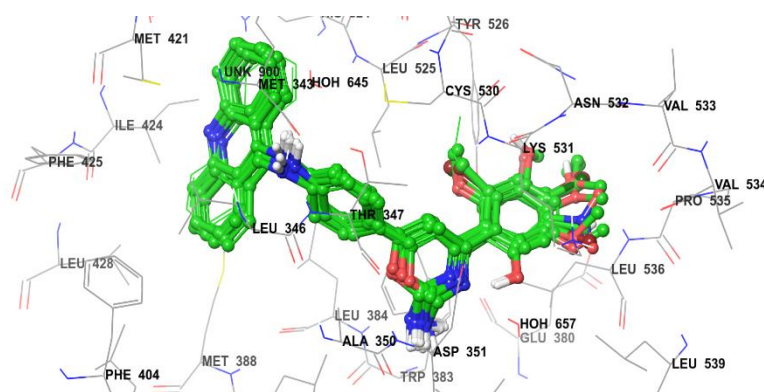
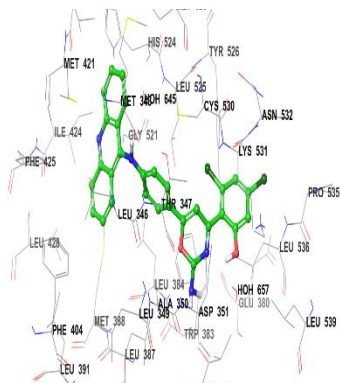


**Figure 3.** Docked poses of all compounds 1a-z with ER $\alpha$  (2IOG)

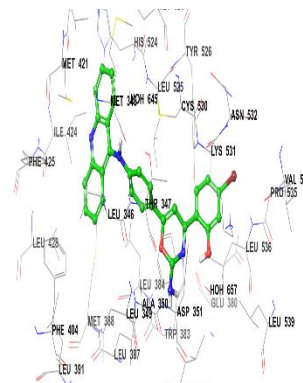
Compound 1x (G Score: -12.91)

Compound 1u (G Score: -12.84)





Compound 1r (G Score: -11.83)



Compound 1s (G Score: -11.31)

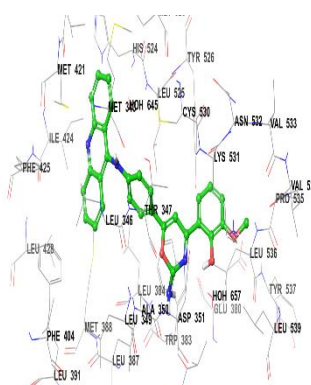
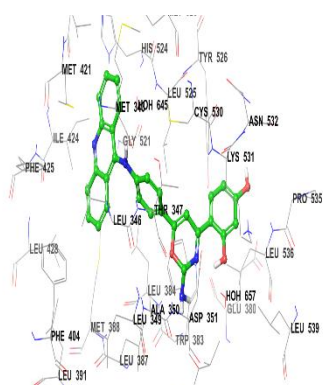


**Figure 4.** Best affinity mode of docked compounds with ER $\alpha$  (2IOG)

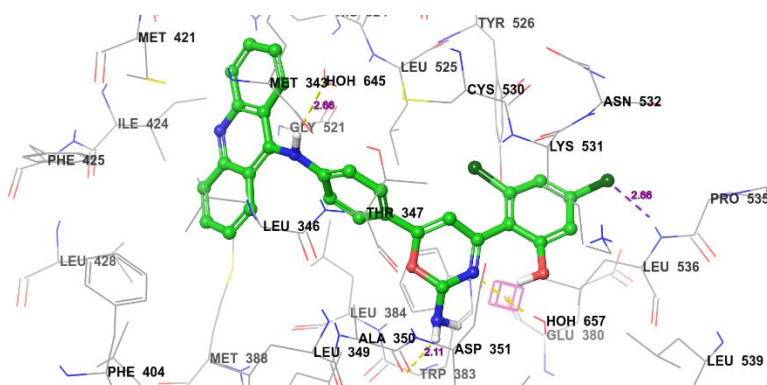


**Figure 5.** Hydrogen bonding interaction of compound 1x with ER $\alpha$  (2IOG)

By applying the qikprop module of the Schrodinger suite 2019-4, the ADMET properties for the designed ligands 1a–z (Table 2) can be predicted in silico. To comprehend the molecular insights involved in binding of 1x in the active pocket of

2IOG, a 100-ns molecular dynamic simulation was conducted. The RMSD of the protein C, backbone, and heavy atoms was observed in the range of 1.6-4.2 and 1.50-3.50 from the derived trajectory analysis, respectively (Figure 6). The Ca atoms varied between 1.5 and 4.2 before stabilising 55 ns into the run with a 3.0 RMSD. At 42 ns, greater RMSD variations (up to 4.2 ) were seen. Stable hydrophobic interactions with ALA 350, TRP 383, PHE 404, LEU 525, and LYS 531 were seen during simulation. 30 ligand interactions with amino acids of the protein were made in total, ranging from MET 343 to THR 347, LEU 349 to PHE 404, and MET 421 to LEU 536. The majority of the hydrophobic interactions (5%–90% of simulated time) between the ligand and the ALA 350 residues stabilise the ligand. Over the duration of 10% to 65% of the simulation trajectory, it additionally established hydrogen bonds with THR 347, ALA 350, ASP 351, and VAL 533. The chronology of connections between proteins and ligands is shown. The MD trajectory posture preserves the hydrogen bond created by the docking pose with LYS 531, VAL 533, ASP 351, and VAL 534, according to the 2D-trajectory interaction diagram (Figure 7). The nitrogen of the acridine ring accepted one hydrogen bond with VAL 533 and LYS 531 through the water molecule with 32% and 11%, respectively, of the entire simulation period. The amino group in compound A38 donated one hydrogen bond to THR 347 with 33%. The amino group accepted hydrogen bonds from VAL 534 and TRP 383 with 15% and 50% of the total simulation period, respectively, and the nitrogen of the oxazine ring accepted one hydrogen bond from VAL 534. Acridine had a 50% pi-pi stacking with TRP 383.

**Table 2.** *In-silico* ADMET screening for proposed compounds (1a-z)

| Compound | Mol.Wt  | Do nor HB | Accept HB | QPlog HERG | metab | QPlog Khsa | % Human Oral Absorption | Rule of Five |
|----------|---------|-----------|-----------|------------|-------|------------|-------------------------|--------------|
| 1a       | 521.415 | 3         | 4.5       | -8.953     | 3     | 1.261      | 80.034                  | 2            |
| 1b       | 521.415 | 3         | 4.5       | -8.903     | 3     | 1.264      | 81.057                  | 2            |
| 1c       | 521.415 | 3         | 4.5       | -8.946     | 3     | 1.273      | 80.503                  | 2            |
| 1d       | 456.546 | 3         | 4.5       | -8.833     | 4     | 1.261      | 93.133                  | 1            |
| 1e       | 456.546 | 3         | 4.5       | -8.913     | 4     | 1.291      | 91.921                  | 1            |
| 1f       | 456.546 | 3         | 4.5       | -8.875     | 4     | 1.282      | 92.478                  | 1            |
| 1g       | 472.545 | 3         | 5.25      | -8.973     | 4     | 1.179      | 91.454                  | 1            |

|                    |         |     |      |        |       |          |                              |       |
|--------------------|---------|-----|------|--------|-------|----------|------------------------------|-------|
| 1h                 | 472.545 | 3   | 5.25 | -8.948 | 4     | 1.156    | 90.787                       | 1     |
| 1i                 | 472.545 | 3   | 5.25 | -8.92  | 4     | 1.162    | 90.83                        | 1     |
| 1j                 | 460.509 | 3   | 4.5  | -8.887 | 3     | 1.165    | 91.998                       | 1     |
| 1k                 | 460.509 | 3   | 4.5  | -8.898 | 3     | 1.176    | 91.507                       | 1     |
| 1l                 | 487.517 | 3   | 5.5  | -8.898 | 4     | 1.102    | 83.089                       | 0     |
| 1m                 | 458.518 | 4   | 5.25 | -8.884 | 4     | 0.915    | 89.14                        | 0     |
| 1n                 | 470.573 | 3   | 4.5  | -8.895 | 4     | 1.387    | 94.529                       | 1     |
| 1o                 | 486.572 | 3   | 5.25 | -8.917 | 4     | 1.278    | 96.49                        | 1     |
| 1p                 | 486.572 | 3   | 5.25 | -9.111 | 4     | 1.289    | 93.871                       | 1     |
| 1q                 | 511.409 | 3   | 4.5  | -8.797 | 3     | 1.35     | 82.533                       | 2     |
| 1r                 | 474.518 | 5   | 6    | -8.798 | 5     | 0.695    | 77.876                       | 0     |
| 1s                 | 488.545 | 4   | 6    | -8.709 | 5     | 0.937    | 94.858                       | 0     |
| 1t                 | 537.414 | 4   | 5.25 | -8.691 | 4     | 1.021    | 81.857                       | 1     |
| 1u                 | 537.414 | 4   | 5.25 | -8.725 | 4     | 1.028    | 70.585                       | 2     |
| 1v                 | 537.414 | 4   | 5.25 | -8.725 | 4     | 1.028    | 70.576                       | 2     |
| 1w                 | 502.571 | 3   | 6    | -8.748 | 5     | 1.184    | 80.182                       | 2     |
| 1x                 | 527.409 | 4   | 5.25 | -8.663 | 4     | 1.121    | 70.725                       | 2     |
| 1y                 | 490.991 | 3   | 4.5  | -8.639 | 4     | 1.367    | 96.817                       | 1     |
| 1z                 | 532.598 | 3   | 6.75 | -8.43  | 6     | 1.162    | 80.494                       | 2     |
| Recommended values | 130-725 | 0-6 | 2-20 | -2-6.5 | 1 – 8 | -1.5-1.5 | >80% is high<br><25% is poor | max 4 |

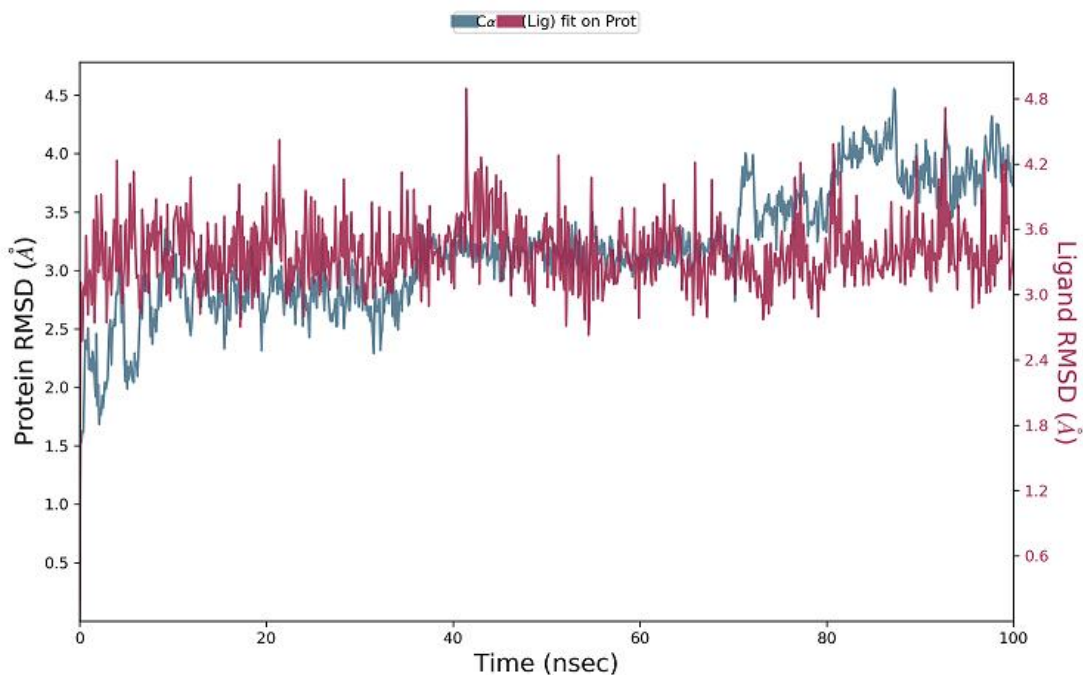


**Figure 6.** Protein- Ligand RMSD of 1x

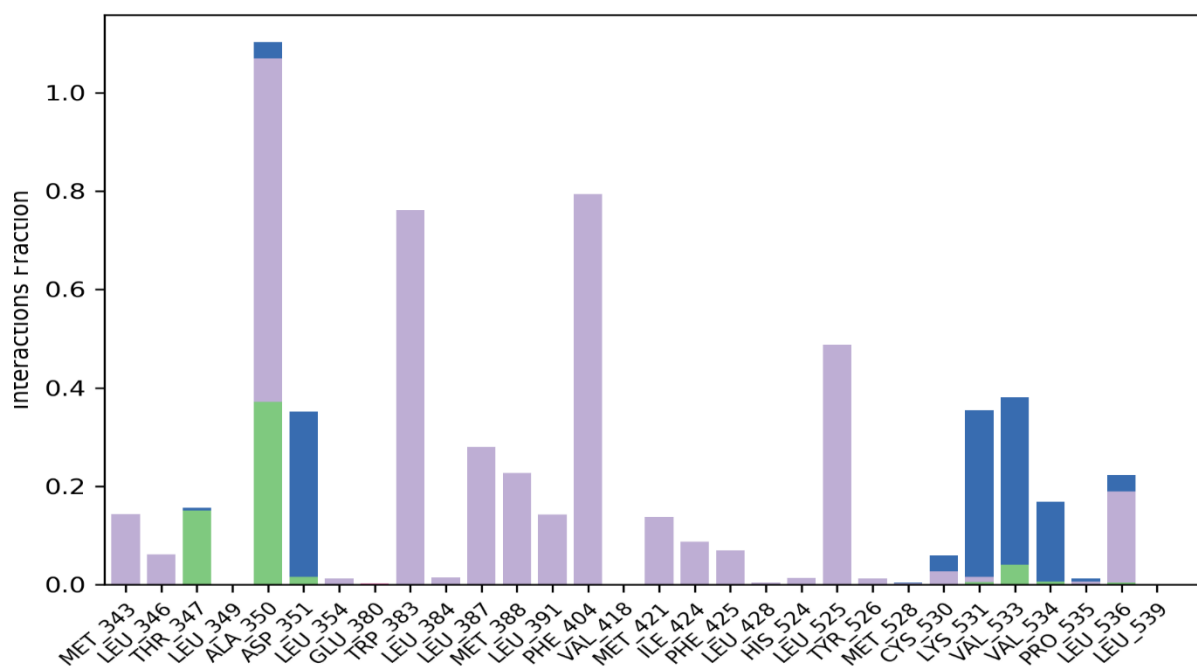


**Figure 7.** Protein-Ligand contacts of 1x histogram

Moreover, MM-GBSA free restricting vitality, known as the target for the ER, was used to assess molecular docking (PDB ID: 2IOG). The scoring function's projected lowest energy poses are examined to show how accurate docking is. The Glide scores and the experimental binding mode discovered by X-ray crystallography are almost identical to one another. The

Glide score and MM-GBSA free energy values are produced by the docking of ligands into the coupling pocket. The subtleties of the MM-GBSA free restricting vitality for the compounds **1a-z** are shown in (Table 3).

**Table 3.** Binding free energy calculations using Prime MM/GBSA Approach.

| Compound | $\Delta G$ bind (Kcal/mol) | $\Delta G$ bind Coulomb | $\Delta G$ bind covalent | $\Delta G$ bind H Bond | $\Delta G$ bind Lipophilic |
|----------|----------------------------|-------------------------|--------------------------|------------------------|----------------------------|
| 1x       | -68.69                     | 49.24                   | -1.09                    | 3.75                   | -34.57                     |
| 1u       | -64.81                     | 20.37                   | 13.36                    | 0.97                   | -34.68                     |
| 1r       | -71.17                     | -1.79                   | 12.63                    | 0.64                   | -32.68                     |
| 1s       | -48.73                     | 41.19                   | 5.95                     | 1.84                   | -35.19                     |
| 1n       | -51.76                     | 22.93                   | 5.77                     | 2.73                   | -33.41                     |
| 1c       | -66.15                     | 1.97                    | 6.87                     | 1.51                   | -33.77                     |
| 1p       | -78.35                     | 9.86                    | 16.68                    | -0.02                  | -40.17                     |
| 1k       | -60.94                     | 16.56                   | 7.39                     | 3.22                   | -34.27                     |
| 1h       | -61.66                     | 39.89                   | 8.41                     | 4.93                   | -36.24                     |
| 1f       | -71.3                      | 6.31                    | 13.41                    | 2.48                   | -39.9                      |
| 1g       | -64.86                     | 12.2                    | 9.84                     | 3.47                   | -39.52                     |
| 1i       | -66.28                     | 41.66                   | -8.82                    | 3.67                   | -33.41                     |
| 1y       | -69                        | 12.45                   | 15.47                    | 1.94                   | -41.86                     |
| 1m       | -62.79                     | 17.95                   | 8.98                     | 0.69                   | -40.14                     |
| 1j       | -64.73                     | 16.9                    | 9.33                     | -0.11                  | -34.2                      |
| 1a       | -65.25                     | 8.65                    | 3.13                     | 1.35                   | -32.45                     |
| 1e       | -59.15                     | 39.49                   | 10.6                     | 2.38                   | -36.82                     |
| 1v       | -38.81                     | 41.92                   | 12.58                    | 2.74                   | -33.58                     |
| 1d       | -62.07                     | 27.98                   | 4.8                      | 0.27                   | -36.95                     |
| 1z       | -63.71                     | 29.87                   | -7.03                    | 2.72                   | -34.93                     |
| 1t       | -65.21                     | 24.44                   | 4.73                     | 1.48                   | -32.8                      |
| 1o       | -68.66                     | 24.85                   | 4.29                     | 0.91                   | -34.2                      |
| 1b       | -62.13                     | 53.63                   | 2.02                     | 2.88                   | -34.46                     |
| 1l       | -47.52                     | 28.06                   | 10.86                    | 2.19                   | -34.19                     |

## CONCLUSION

We employed advanced in-silico and coupled molecular modelling approaches to discover 9- aniline acridine based novel ER $\alpha$  small molecule inhibitors in this investigation. From the Specs-SC small molecule database, 5467 molecules containing 9-anilino acridine were selected for this study. The top-docking pose of one hit from the molecular docking screening of these drugs against the ER $\alpha$  target was then used in a lengthy (100 ns) MD simulation. All ligands underwent MM/GBSA binding free energy calculations. The FDA-approved ER $\alpha$  inhibitors went through the same procedure. In this study, we made use of text mining techniques, which quickly and efficiently decrease the total number of compounds in huge small molecule datasets to manageable amounts for additional investigation. The statistical data gathered indicates that the model has good accuracy and predictive power. The model predicts the likelihood that tested drugs will have therapeutic efficacy with normalised values between 0 and 1 (active) (active). The Cancer QSAR model in MC/MD shows that 1x has a therapeutic activity potential of 0.60. It was found that this chemical is not harmful in any of the 26 distinct toxicity models that it was evaluated in. Finally, throughout this rigorous combination screening, we looked for drugs that may be used to inhibit ER $\alpha$  activity. This innovative scaffold might open the door to the creation of tiny ER $\alpha$  inhibitors.

## ACKNOWLEDGMENT

The authors would like to acknowledge the generous research infrastructure and supports from JSS College of Pharmacy, JSS Academy of Higher Education & Research, Rocklands, Ooty, The Nilgiris, Tamilnadu, India.

## CONFLICT OF INTEREST

The authors declare that there is no conflict of interest.

## AUTHORS CONTRIBUTION

P.V.K. and K.R. collected the literature and arranged the References. Prepared study concept and designed. P.V.K. and K.R. performed molecular modelling part. K.R. A.B. K.R. G.B. critically analysed the data. P.V.K. wrote the manuscript. P.V.K. K.R. A.B. K.R. G.B. critically edited the manuscript.

## FUNDING

This Research was funded by JSSAHER, Mysuru. Order no. JSSAHER/REG/RES/JSSURF/29(1)/2010-11 dated 15.11.2021

## DATA AVAILABILITY

Data available at Corresponding author.

## ETHICS STATEMENT

This article does not contain any studies on human participants or animals performed by any of the authors.

## REFERENCES

1. M. Martinez-Archundiaa, J.B. García-Vázquez, B. Colin-Astudilloa, M. Belloa, B. Prestegui-Martela, A. Chavez-Blancoa, et al. Development of leads targeting ER- $\alpha$  in breast cancer: An *in silico* exploration from natural domain. *Anti-Cancer Agents in Medicinal Chemistry*. 2018; 131: 14-22.
2. Janea Myles D. Dela Cruz<sup>1</sup>, Sophia Allison A. Dones<sup>1</sup>, Rianne C. Villanueva<sup>1</sup>, Alexis M. Labrador<sup>1</sup>, Myla R. Santiago-Bautista<sup>1</sup>. Molecular Docking and *in silico* Pharmacological Screening of Oleosin from *Cocos Nucifera* Complexed with Tamoxifen in Developing Potential Breast Chemotherapeutic Leads. *Asian Pac J Cancer Prev*, 2022; 23 (7): 2421-2430.
3. Vraj Shah, Jaydip Bhaliya, Gautham M. Patel, *In silico* docking and ADME study of deketene curcumin derivatives (DKC) as an aromatase inhibitor or antagonist to the estrogen-  $\alpha$  positive receptor (ER $\alpha$ ): potent application of breast cancer. *Structural Chemistry*, 2022; 33: 571-600.
4. Snehal S. Ashtekar, Neela M. Bhatia, Manish S. Bhatia. Development of leads targeting ER- $\alpha$  in breast cancer: An *in silico* exploration from natural domain. *Steroids*, 2018; <https://doi.org/10.1016/j.steroids.2017.12.016>.
5. Rajagopal Kalirajan, Sundaram Sankar, Selvaraj Jubie, Byran Gowramma. Molecular Docking studies and *in-silico* ADMET Screening of Some novel Oxazine substituted 9-Anilinoacridines as Topoisomerase II Inhibitors. *Indian Journal of Pharmaceutical Education and Research*, 2017; 51:1.

6. El Mehdi Bouricha, Mohammed Hakmi , Jihane Akachar , Fouad Zouaidia, Azeddine Ibrahimi. *In-silico* identification of potential inhibitors targeting the DNA binding domain of estrogen receptor  $\alpha$  for the treatment of hormone therapy-resistant breast cancer. *Journal of Biomolecular Structure and Dynamics*, 2021; DOI: 10.1080/07391102.2020.1869094.
7. Divya B, Fuqiang B, Paul S. R, Kriti S and Artem C. Computer-Aided Ligand Discovery for Estrogen Receptor Alpha. *Int. J. Mol. Sci*, 2020; 21: 4193.
8. Rajagopal Kalirajan<sup>1</sup>, Arumugasamy Pandiselvi<sup>1</sup>, Byran Gowramma<sup>1</sup>, Pandiyan Balachandran. In-silico Design, ADMET Screening, MM-GBSA Binding Free Energy of Some Novel Isoxazole Substituted 9-Anilinoacridines as HER2 Inhibitors Targeting Breast Cancer. *Current Drug Research Reviews*, 2019; 11: 2.
9. Alamgir Hossain. Molecular Docking, Drug-Likeness and ADMET Analysis, Application of Density Functional Theory (DFT) and Molecular Dynamics (MD) Simulation to the Phytochemicals from *Withania Somnifera* as Potential Antagonists of Estrogen Receptor Alpha (ER-  $\alpha$ ). *Current Computer-Aided Drug Design*, 2021; 17:797-805.
10. Baliwada Aparna, Kalirajan Rajagopal, Potlapati Varakumar, Kannan Raman, Gowramma Byran, Srikanth Jupudi. Identifying new 9-anilinoacridine-based parp1 inhibitors using text mining and integrated molecular modeling approaches. *Eur. Chem. Bull*, 2022; 11(5): 22 – 30.
11. Jesudass Joseph Sahayarayan, Kulanthaivel Soundar Rajan, Ramasamy Vidhyavathi, Mutharasappan Nachiappan, Dhamodharan Prabhu, Saleh Alfarraj et al. In-silico protein-ligand docking studies against the estrogen protein of breast cancer using pharmacophore based virtual screening approaches. *Saudi Journal of Biological Sciences*, 2021; 28: 400-407.



12. Gurubasavaraj Swamy Purawarga Matada , Prasad Sanjay Dhiwar , Nahid Abbas , Ekta Singh , Abhishek Ghara , Arka Das et al. Molecular docking and molecular dynamic studies: screening of phytochemicals against EGFR, HER2, estrogen and NF-KB receptors for their potential use in breast cancer. *Journal of Biomolecular Structure and Dynamics*, 2021; DOI: 10.1080/07391102.2021.1877823.
13. V.L. Maruthanila, R. Elancheran, Nand Kishor Roy, Anupam Bhattacharya, Ajaikumar B. Kunnumakkara, S. kabilan et al. *In Silico* Molecular Modelling of Selected Natural Ligands and their Binding Features with Estrogen Receptor Alpha. *Current Computer-Aided Drug Design*, 2019; 15: 89-96.

**Table 1.** Docking studies for Compounds 1a-z with ER $\alpha$  (2IOG)

| Compound        | Glide score | Lipophilic EVdW | Phob En | H Bond | XP Electro | Low MW | XP Penalties | Rot penal |
|-----------------|-------------|-----------------|---------|--------|------------|--------|--------------|-----------|
| 1x              | -12.91      | -8.92           | -2.7    | -0.67  | -0.35      | 0      | 0            | 0.13      |
| 1u              | -12.84      | -8.87           | -2.7    | -0.67  | -0.33      | 0      | 0            | 0.12      |
| 1r              | -11.83      | -8.42           | -2.2    | -0.65  | -0.32      | 0      | 0            | 0.15      |
| 1s              | -11.31      | -7.36           | -2.7    | -0.63  | -0.34      | 0      | 0            | 0.15      |
| 1n              | -10.51      | -9.16           | -2.7    | -0.55  | -0.2       | 0      | 2.4          | 0.16      |
| 1c              | -10.37      | -8.9            | -2.7    | -0.58  | -0.28      | 0      | 2.4          | 0.13      |
| 1p              | -10.31      | -9.11           | -2.7    | -0.42  | -0.22      | 0      | 2.4          | 0.18      |
| 1k              | -10.17      | -8.43           | -2.7    | -0.53  | -0.26      | 0      | 2.4          | 0.16      |
| 1h              | -10.12      | -8.65           | -2.7    | -0.49  | -0.34      | 0      | 2.4          | 0.16      |
| 1f              | -10.08      | -8.78           | -2.7    | -0.54  | -0.2       | 0      | 2.4          | 0.17      |
| 1g              | -9.88       | -8.32           | -2.7    | -0.7   | -0.29      | 0      | 2.4          | 0.16      |
| 1i              | -9.84       | -8.91           | -2.7    | -0.05  | -0.26      | 0      | 2.4          | 0.16      |
| 1y              | -9.78       | -8.94           | -2.7    | -0.04  | -0.2       | 0      | 2.4          | 0.14      |
| 1m              | -9.63       | -8.4            | -2.7    | -0.32  | -0.29      | 0      | 2.4          | 0.16      |
| 1j              | -9.44       | -8.43           | -2.7    | -0.11  | -0.14      | 0      | 2.4          | 0.16      |
| 1a              | -9.39       | -8.51           | -2.7    | -0.14  | -0.13      | 0      | 2.4          | 0.13      |
| 1e              | -9.38       | -8.6            | -2.7    | 0      | -0.16      | 0      | 2.4          | 0.17      |
| 1v              | -9.37       | -7.77           | -2.7    | -0.68  | -0.26      | 0      | 2.4          | 0.12      |
| 1d              | -9.17       | -8.36           | -2.7    | -0.09  | -0.14      | 0      | 2.4          | 0.17      |
| 1z              | -9.11       | -8.38           | -2.7    | -0.7   | -0.43      | 0      | 3.4          | 0.12      |
| 1t              | -9.04       | -8.08           | -2.7    | -0.06  | -0.18      | 0      | 2.4          | 0.12      |
| 1o              | -8.83       | -8.02           | -2.7    | 0      | -0.07      | 0      | 2.4          | 0.18      |
| 1b              | -8.26       | -7.54           | -2.7    | 0      | -0.11      | 0      | 2.4          | 0.13      |
| 1l              | -6.8        | -8.47           | -2.7    | 0      | -0.07      | 0      | 4.8          | 0.15      |
| Tamoxifen (Std) | -11.58      | -8.97           | -2.7    | 0      | -0.06      | -0.26  | 0            | 0.42      |
| Ledacrine (Std) | -7.93       | -5.68           | -2.14   | 0      | 0          | -0.42  | 0            | 0.31      |

**Table 2.** *In-silico* ADMET screening for proposed compounds (1a-z)

| Compound           | Mol.Wt  | Do nor HB | Accept HB | QPlog HERG | metab | QPlog Khsa | % Human Oral Absorption      | Rule of Five |
|--------------------|---------|-----------|-----------|------------|-------|------------|------------------------------|--------------|
| 1a                 | 521.415 | 3         | 4.5       | -8.953     | 3     | 1.261      | 80.034                       | 2            |
| 1b                 | 521.415 | 3         | 4.5       | -8.903     | 3     | 1.264      | 81.057                       | 2            |
| 1c                 | 521.415 | 3         | 4.5       | -8.946     | 3     | 1.273      | 80.503                       | 2            |
| 1d                 | 456.546 | 3         | 4.5       | -8.833     | 4     | 1.261      | 93.133                       | 1            |
| 1e                 | 456.546 | 3         | 4.5       | -8.913     | 4     | 1.291      | 91.921                       | 1            |
| 1f                 | 456.546 | 3         | 4.5       | -8.875     | 4     | 1.282      | 92.478                       | 1            |
| 1g                 | 472.545 | 3         | 5.25      | -8.973     | 4     | 1.179      | 91.454                       | 1            |
| 1h                 | 472.545 | 3         | 5.25      | -8.948     | 4     | 1.156      | 90.787                       | 1            |
| 1i                 | 472.545 | 3         | 5.25      | -8.92      | 4     | 1.162      | 90.83                        | 1            |
| 1j                 | 460.509 | 3         | 4.5       | -8.887     | 3     | 1.165      | 91.998                       | 1            |
| 1k                 | 460.509 | 3         | 4.5       | -8.898     | 3     | 1.176      | 91.507                       | 1            |
| 1l                 | 487.517 | 3         | 5.5       | -8.898     | 4     | 1.102      | 83.089                       | 0            |
| 1m                 | 458.518 | 4         | 5.25      | -8.884     | 4     | 0.915      | 89.14                        | 0            |
| 1n                 | 470.573 | 3         | 4.5       | -8.895     | 4     | 1.387      | 94.529                       | 1            |
| 1o                 | 486.572 | 3         | 5.25      | -8.917     | 4     | 1.278      | 96.49                        | 1            |
| 1p                 | 486.572 | 3         | 5.25      | -9.111     | 4     | 1.289      | 93.871                       | 1            |
| 1q                 | 511.409 | 3         | 4.5       | -8.797     | 3     | 1.35       | 82.533                       | 2            |
| 1r                 | 474.518 | 5         | 6         | -8.798     | 5     | 0.695      | 77.876                       | 0            |
| 1s                 | 488.545 | 4         | 6         | -8.709     | 5     | 0.937      | 94.858                       | 0            |
| 1t                 | 537.414 | 4         | 5.25      | -8.691     | 4     | 1.021      | 81.857                       | 1            |
| 1u                 | 537.414 | 4         | 5.25      | -8.725     | 4     | 1.028      | 70.585                       | 2            |
| 1v                 | 537.414 | 4         | 5.25      | -8.725     | 4     | 1.028      | 70.576                       | 2            |
| 1w                 | 502.571 | 3         | 6         | -8.748     | 5     | 1.184      | 80.182                       | 2            |
| 1x                 | 527.409 | 4         | 5.25      | -8.663     | 4     | 1.121      | 70.725                       | 2            |
| 1y                 | 490.991 | 3         | 4.5       | -8.639     | 4     | 1.367      | 96.817                       | 1            |
| 1z                 | 532.598 | 3         | 6.75      | -8.43      | 6     | 1.162      | 80.494                       | 2            |
| Recommended values | 130-725 | 0-6       | 2-20      | -2-6.5     | 1 – 8 | -1.5-1.5   | >80% is high<br><25% is poor | max 4        |

**Table 3.** Binding free energy calculations using Prime MM/GBSA Approach.

| Compound | $\Delta G$ bind (Kcal/mol) | $\Delta G$ bind Coulomb | $\Delta G$ bind covalent | $\Delta G$ bind H Bond | $\Delta G$ bind Lipophilic |
|----------|----------------------------|-------------------------|--------------------------|------------------------|----------------------------|
| 1x       | -68.69                     | 49.24                   | -1.09                    | 3.75                   | -34.57                     |
| 1u       | -64.81                     | 20.37                   | 13.36                    | 0.97                   | -34.68                     |
| 1r       | -71.17                     | -1.79                   | 12.63                    | 0.64                   | -32.68                     |
| 1s       | -48.73                     | 41.19                   | 5.95                     | 1.84                   | -35.19                     |
| 1n       | -51.76                     | 22.93                   | 5.77                     | 2.73                   | -33.41                     |
| 1c       | -66.15                     | 1.97                    | 6.87                     | 1.51                   | -33.77                     |
| 1p       | -78.35                     | 9.86                    | 16.68                    | -0.02                  | -40.17                     |
| 1k       | -60.94                     | 16.56                   | 7.39                     | 3.22                   | -34.27                     |
| 1h       | -61.66                     | 39.89                   | 8.41                     | 4.93                   | -36.24                     |
| 1f       | -71.3                      | 6.31                    | 13.41                    | 2.48                   | -39.9                      |
| 1g       | -64.86                     | 12.2                    | 9.84                     | 3.47                   | -39.52                     |
| 1i       | -66.28                     | 41.66                   | -8.82                    | 3.67                   | -33.41                     |
| 1y       | -69                        | 12.45                   | 15.47                    | 1.94                   | -41.86                     |
| 1m       | -62.79                     | 17.95                   | 8.98                     | 0.69                   | -40.14                     |
| 1j       | -64.73                     | 16.9                    | 9.33                     | -0.11                  | -34.2                      |
| 1a       | -65.25                     | 8.65                    | 3.13                     | 1.35                   | -32.45                     |
| 1e       | -59.15                     | 39.49                   | 10.6                     | 2.38                   | -36.82                     |
| 1v       | -38.81                     | 41.92                   | 12.58                    | 2.74                   | -33.58                     |
| 1d       | -62.07                     | 27.98                   | 4.8                      | 0.27                   | -36.95                     |
| 1z       | -63.71                     | 29.87                   | -7.03                    | 2.72                   | -34.93                     |
| 1t       | -65.21                     | 24.44                   | 4.73                     | 1.48                   | -32.8                      |
| 1o       | -68.66                     | 24.85                   | 4.29                     | 0.91                   | -34.2                      |
| 1b       | -62.13                     | 53.63                   | 2.02                     | 2.88                   | -34.46                     |
| 1l       | -47.52                     | 28.06                   | 10.86                    | 2.19                   | -34.19                     |

## Figures

**Figure 1.** Structure of compounds 1a-z

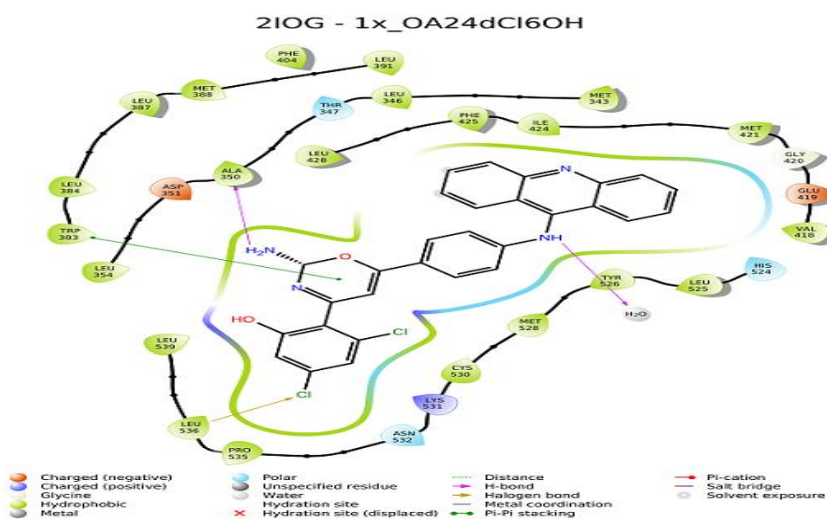


**Figure 2.** Ligand interaction of compound 1x with ER $\alpha$  (2IOG)

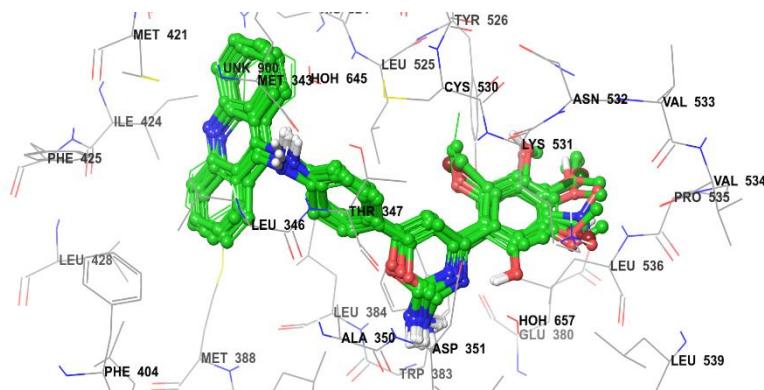
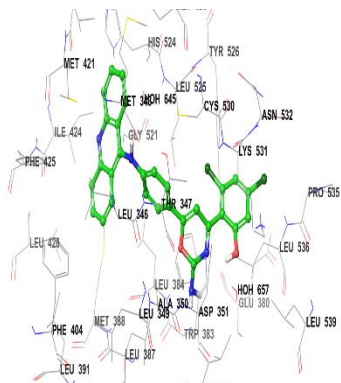


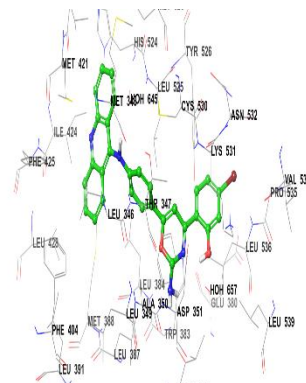
**Figure 3.** Docked poses of all compounds 1a-z with ER $\alpha$  (2IOG)

Compound 1x (G Score: -12.91)

Compound 1u (G Score: -12.84)



Compound 1r (G Score: -11.83)



Compound 1s (G Score: -11.31)

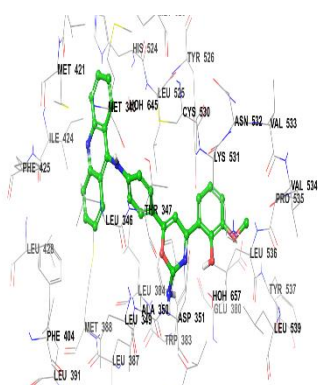
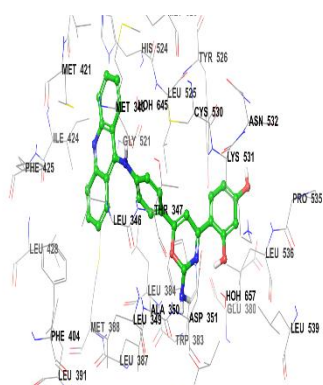


**Figure 4.** Best affinity mode of docked compounds with ER $\alpha$  (2IOG)

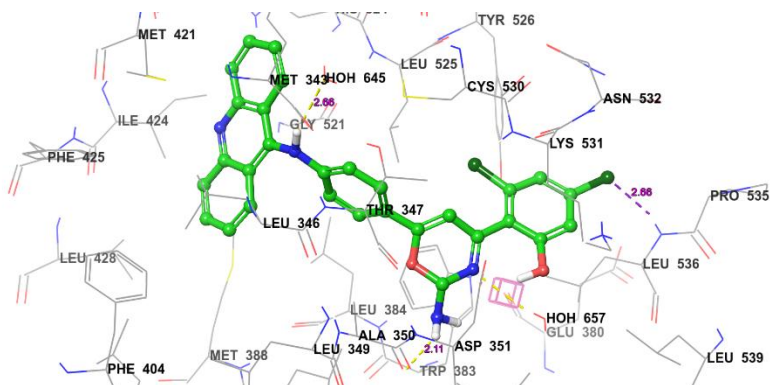


**Figure 5.** Hydrogen bonding interaction of compound 1x with ER $\alpha$  (2IOG)

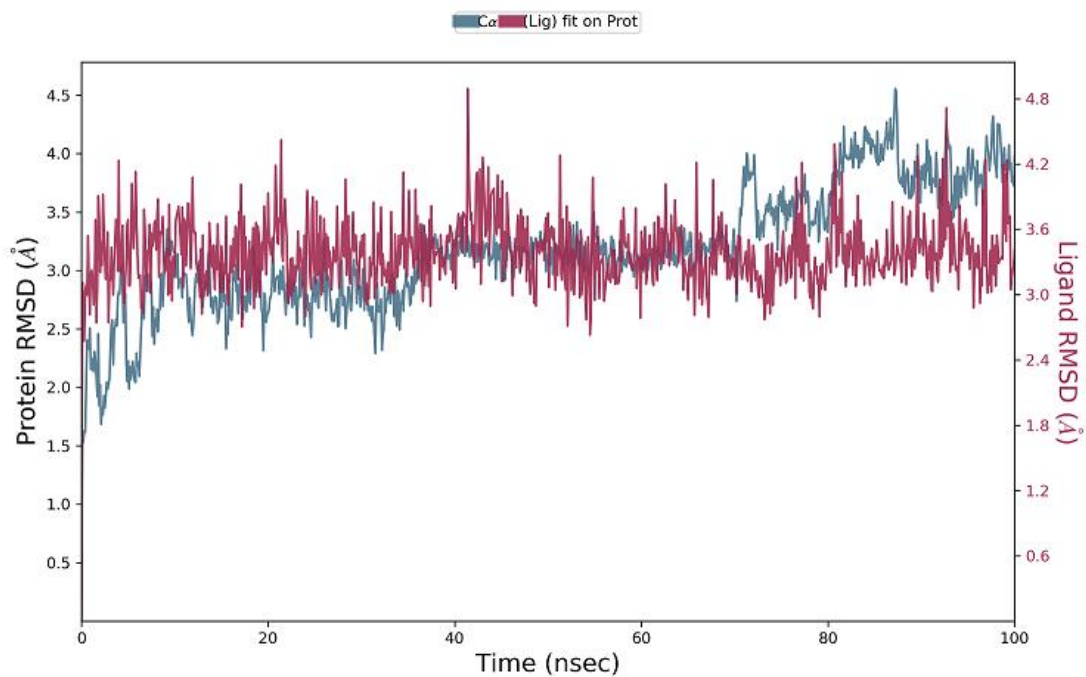


**Figure 6.** Protein- Ligand RMSD of 1x

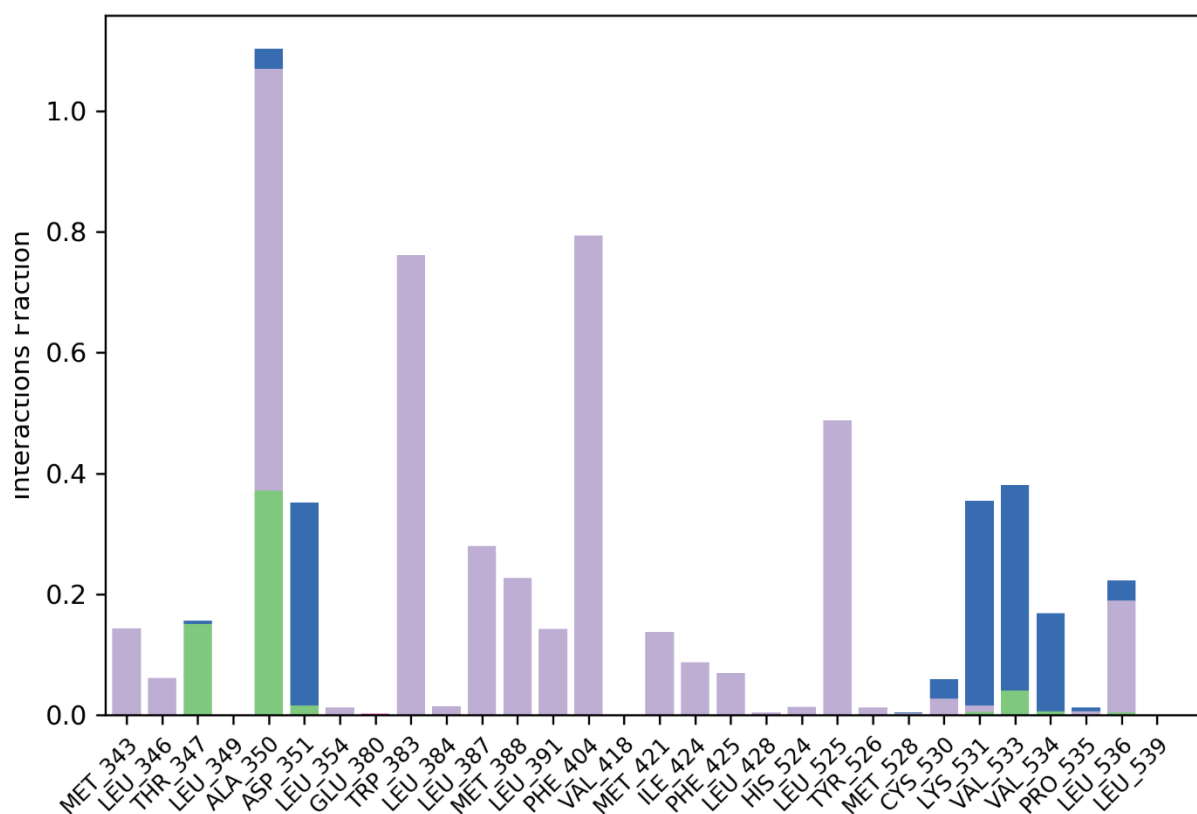


**Figure 7.** Protein-Ligand contacts of 1x histogram